**ORIGINAL PAPER**

# Microwave Pretreatment for the Improvement of Physicochemical Properties of Carob Flour and Rice Starch–Based Electrospun Nanofilms

Eylul Uygun[1] · Eda Yildiz[1] · Gulum Sumnu[1] · Serpil Sahin[1]

## Abstract

The aim of this study was to determine the effects of microwave pretreatment on physicochemical characteristics of carob flour and rice starch–based nanofibers produced by electrospinning. The effects of microwave heating on production of nanofibers by electrospinning have not been studied before. Another aim of the study was to fabricate and characterize nanofibers by using different carob flour concentrations (3%, 5% w/v) and rice starch (0.5% w/v). Films were characterized by scanning electron microscopy, water vapor permeability, X-ray diffraction, mechanical test, differential scanning calorimeter, and Fourier transform infrared spectrophotometer. Homogenous and bead-free fibers were obtained when microwave heating was used. Nanofibers originated from microwave-heated solution presented better characteristics in terms of water vapor permeability and mechanical properties as compared with conventionally heated ones. Microwave-heated solution had higher viscosity and available amino group amount as compared with conventionally heated solution. This study showed that microwave heating can be considered as a promising pretreatment method for electrospinning rather than conventional heating to be used in food packaging area.

**Keywords** Packaging · Legume flour · Biodegradable · Electromagnetic heating

## Introduction

It is a known fact that nanoscale fibers give promising results in many fields such as enzyme immobilization, drug delivery, textile production, biosensors, and tissue engineering. Among nanofiber formation methods, electrospinning is one of the commonly used ones (Li and Xia 2004). Electrospinning is quite advantageous in terms of its cost and simplicity. It is also possible to produce well-ordered, homogeneous, and more porous fibers with larger surface to volume ratio by electrospinning (Hadad et al. 2019). In nanofiber formation, it is possible to use synthetic, natural, and hybrid materials. As a natural source, gelatin, collagen, soy, casein, gliadin, zein, and whey were preferred as proteins. In addition to that, cellulose, chitosan, starch, pullulan, cyclodextrin, and alginate were used as polysaccharides (Mendes et al. 2017). Using of natural sources is also important in terms of producing environmentally friendly films. There is a growing interest in using biodegradable products, which are less waste and, thus, sustainable (Fabra et al. 2015).

Flours can also be used as a natural source for nanofiber formation since they contain carbohydrates, proteins, fats, and fibers. In recent years, flours such as lentil and pea flours are used to produce nanofibers by electrospinning (Tam et al. 2017; Oguz et al. 2018). Among natural flours, carob flour is differentiated from others by its high fiber (7.3–9.61%) and total sugar content (38–56%). It also contains protein (3–5%) (Özcan et al. 2007; Yousif and Alghzawi 2000). High fiber content of carob flour may bring some benefits in mechanical properties of nanofiber films. It was found that fiber addition

✉ Gulum Sumnu
  gulum@metu.edu.tr

  Eylul Uygun
  eylul.uygun@metu.edu.tr

  Eda Yildiz
  edaberk@metu.edu.tr

  Serpil Sahin
  serp@metu.edu.tr

1   Department of Food Engineering, Middle East Technical University, 06800 Ankara, Turkey

to starch containing electrospinning solutions resulted in an increase in tensile strength and modulus of elasticity of the obtained films (Müller et al. 2009). Therefore, carob flour can be good choice for obtaining electrospun nanofibers with better mechanical properties. There is no study so far in literature about production of carob flour–based nanofibers by electrospinning.

In literature, granule size of potato, tapioca, and corn starches were recorded as 38.3, 19.5, and 17.8 μm, respectively. As different from these starches, granule size of rice starch was indicated as 6.4 μm (Li and Yeh 2001). In this study, rice starch was preferred because it has the lowest granule size and since it was found that films made with starches having smaller size showed better mechanical properties in terms of tensile strength and elongation rate as compared with high granule size starch in polyethylene films (Lim et al. 1992).

To provide better spinnability, addition of a synthetic polymer can be considered. Polyethylene oxide (PEO) is a biodegradable, biocompatible, and water-soluble polymer, which is widely used in electrospinning process. It has high polar affinity and capability of preserving organization. Also, its oxygen atoms have high electron donor power, which enables them to form multiple intramolecular coordinate bonds with cations (Surov et al. 2018).

In this study, to prepare electrospinning solutions, as a pretreatment, microwave heating was selected. Microwave heating is known to provide transfer of energy through the materials in a rapid rate, which reduces processing time significantly. Other advantages of microwave heating over conventional heating are precise process control and selective and volumetric heating. (Sumnu 2001). Moreover, microwaves can change some functional properties of carbohydrates and proteins. It was observed that microwave heating caused changes in structures and properties of potato and tapioca starches. After microwave application, potato starch shifted from Type B to Type A. Microwave heating completely disrupted integrity of starch granules, while conventional heating caused only surface gelatinization (Lewandowicz et al. 1997). This could be related to the fact that microwave energy directly affected moisture in starch granules of crystal region, which ended up easy destruction of granules. In another study, microwave heating was shown to increase in tensile strength of edible films formulated by soy protein isolate and zein up to 5–25% (Wang et al. 2016). This result was explained by the fact that microwave heating might have changed the structure of the solutions. It was also reported that the surface of the films obtained by microwave treatment was smoother with less pores. The hypothesis of the study is that usage of microwave in preparation of electrospinning solutions can be a feasible approach as compared with conventional methods in terms of improving physicochemical properties of electrospun nanofibers. However, to the best of our knowledge, there is no study in literature about investigation of the effects of microwave heating on production of nanofibers by electrospinning. In addition, nanofibers based on carob flour and rice starch mixture solutions have not been developed before. Therefore, the aim of this study was to determine the effects of microwave heating on properties of electrospinning solutions and electrospun nanofibers as compared with conventional heating. In addition, the effects of different carob flour concentrations and rice starch addition on production of nanofibers by electrospinning were investigated.

## Materials and Methods

### Materials

Carob flour was obtained from Havancızade Gıda (İstanbul, Turkey). Rice starch was supplied from National Starch Food Innovation (Bridgewater, NJ, USA). Polyethyleneoxide (PEO) with molecular weight of 900 kDa and sodium hydroxide pellets were bought from Sigma Aldrich Chemical Co. (St. Louis, MO, USA). Polyoxyethylene sorbitan monooleate (Tween 80) (density: 1.064 g/cm$^3$, viscosity: 400–620 cps at 25 °C) was obtained from Merck (Darmstadt, Germany).

### Preparation of Solutions

PEO solutions of 2% (w/v) were prepared by dissolving overnight using magnetic stirrer at 400 rpm (Daihan Scientific Co, KR) at room temperature. Carob flour was added at two different concentrations, which were 3% (w/v) and 5% (w/v), and rice starch was added at 0.5% (w/v) concentration into dissolved PEO solution. Solutions were homogenized by using high-speed homogenizer (IKA T25 Digital Ultra-Turrax; IKA®-Werke GmbH & CO. KG, Staufen, Germany) at 9000 rpm for 4 min. Then, pH of the solutions was adjusted 10 by adding 2 M NaOH. To prepare conventionally heated solutions, solutions were heated up to 80 °C in water bath (GFL, Type 1086, Germany). Then, solutions continued to be heated using magnetic stirrer at 750 rpm and 80 °C for 2 h. After that, solutions were cooled down to room temperature. Then, Tween 80 was added at 2% (w/v) as a surfactant. Solutions were stirred again at 750 rpm for 30 min to disperse Tween 80. To prepare microwave heated solutions, solutions were heated by using a microwave oven (Kenwood, New Jersey, USA) for 2.5 min at 416 W, which solution temperature reaches to 80 °C. Power level was determined by IMPI 2-L test (Buffler 1993). This condition was determined by the preliminary experiments. Then, the same procedure for cooling and addition of Tween 80, as in the case of conventional heating, was followed.

## Characterization of Solutions

### Rheological Characterization

Rheological behaviors of the solutions were examined by using a controlled strain rheometer with cup and bob geometry (Kinexus, Malvern Instruments, UK). Shear rate range was selected as 1 to 100 s$^{-1}$. Measurement temperature was selected as 25 °C. The shear stress ($\tau$) values were recorded with respect to shear rate ($\dot{\gamma}$) values. Measurements were replicated for two times.

### Electrical Conductivity Measurement

Electrical conductivity of the solutions was measured by using conductivity meter (Inolab® 7110, Wissenschaftlich-Technische Werkstätten GmbH, Weilheim, Germany) at 25 °C in duplicate.

### Determination of Available Amino Groups

The orthophthalaldehyde (OPA) method was used to quantify available free amino groups. The method was applied as described by Nielsen et al. (2001). Experiments were performed for the solutions containing 3% carob flour concentration. The solution, which was not exposed to any heat treatment, was considered as a control. Conventionally heated and microwave-heated solutions were also analyzed. Solutions were diluted with 1/20 dilution rate by using distilled water prior to analysis. Absorbance values of samples were measured by using UV/VIS Spectrophotometer at 340 nm (Optizen Pop Nano Bio, Mecasys Co. LTD, Korea). Available amino groups' value was determined by taking reference of glysine standard curve of concentration (0.004–0.0004 g/100 mL) versus absorbance at 340 nm. Available amino group concentration was expressed as g/mL in comparison with unheated solution sample.

## Electrospinning

Films were prepared by using electrospinning device (NanoWeb 103, Mavitek, Mersin, Turkey). Prepared solutions were placed in the device by using 5-mL syringes with 11.53 mm inner diameter. Needle of the syringe was placed horizontally on the pump. Positively charged electrode was connected to the needle, and negatively charged electrode was connected to the collector plate. Collector plate was covered with aluminum foil and placed at 30-cm distance from the needle's tip. Flow rate was selected as 0.8 mL/h, and the voltage was set as 12 kV. Experiments were performed at $21 \pm 1\%$ relative humidity and at $20 \pm 1$ °C temperature.

## Characterization of the Films

The films were labeled as M-5F-0.5S, M-5F-0S, M-3F-0.5S, and C-3F-0.5S with the first letter denoting heating type (microwave—M, conventional—C). Notation in the middle referred to carob flour concentration (either 5% or 3% w/v), and the latter one represented rice starch amount (0.5% w/v or 0) in the formulations.

### SEM

Scanning electron microscopy images of the films was taken by using electron microscope (Nova NanoSEM 430, FEI, Oregon) for carrying out analysis of morphological properties of films. Images were taken at 10000× magnification. Nanofiber diameters were measured by using Image J software to obtain diameter range and calculate average diameter of each sample. For each sample, measurements were performed using randomly selected 100 fibers.

### DSC

Thermal analysis of films was performed by using a differential scanning calorimeter (Pyris 6 DSC, PerkinElmer, Massachusetts, USA). An empty pan was used as reference. In each measurement, around 4–5 mg sample was put in aluminum pans. Samples were firstly cooled down to −60 °C and heated up to 100 °C with 10 °C/min heating rate. Glass transition temperatures of films were determined, and measurements were replicated twice.

### Mechanical Test Measurement

Tensile strength, Young's modulus, and percentage elongation at break were determined by using texture analyzer (Brookfield Texture Analyzer CT310K, Middleborough, USA). Measurements were performed by using 0.1 N preload at speed of 25 mm/min. Film samples were prepared in 25 mm width and 80 mm length. At room temperature, experiments were repeated twice.

### FTIR Analysis

Fourier transform infrared (FTIR) spectroscopy analyses of film samples were performed by using a FTIR spectrometer (IR-Affinity1, Shimadzu Corporation, Kyoto, Japan) with Attenuated Total Reflectance (ATR) attachment. Analysis were carried out at 600–4000 cm$^{-1}$ frequency range with 32 number of scans and 4 cm$^{-1}$ resolutions.

## WVP

Water vapor permeability (WVP) of films was determined by following ASTM, E96 standard method (Stand. Test Methods Water Vap. Transm. Mater. 1995). Firstly, thickness of nanofilms was measured with calipers, and 10 measurements were taken for each film sample. Water vapor permeability cups made of plastic with 4 cm diameter were used to perform experiment. Cups were filled with 35 mL water and covered with obtained films. Relative humidity inside the cup was fixed to 100%. Cups were kept in the desiccators. After steady state condition was reached, cups were weighed at 1.5 h intervals for 3 days. Measurements were performed duplicate. Water vapor transmission rate (WVTR) and then water vapor permeability values of the films were calculated. Water vapor transmission rate was calculated from the plot of weight loss versus time graph. Dividing surface area of the cup to the slope of weight loss versus time graph gave water vapor transmission rate. Then, using the Eq. (1) given below, water vapor permeability was calculated;

$$WVP = \frac{WVTR \times \Delta x}{(P_{sat}) \times (R_1 - R_2)} \quad (1)$$

in which WVTR was the water vapor transmission rate (g m$^{-2}$ s$^{-1}$), $P_{sat}$ (kPa) was the saturated vapor pressure at certain temperature, $R_1$ (%) was the relative humidity inside the cup, $R_2$ (%) was the relative humidity outside the cup, and $\Delta x$ (m) was the average thickness of the film.

## XRD

Crystalline property of film samples was examined by X-ray diffractometer (Rigaku Ultima-IV, USA) using copper (Cu) irradiation with 30 mA current and 40 kV energy. Experiments were carried out between 5° and 70° scanning range with 2°/min scanning rate.

## Statistical Analysis

ANOVA was used to make statistical analysis by Minitab software (version 17, State College, PA, USA). If significant difference was found, Tukey's test was used for comparison ($p \leq 0.05$).

## Results and Discussion

### Effects of Heating Method, Carob Flour Concentration, and Starch Addition on Morphology of the Samples

When 3% (w/v) and 5% (w/v) carob flour containing solutions were exposed to conventional heating, homogenous fibers could not be obtained (Fig.1a). On the other hand, homogeneous fibers could be obtained in microwave treated samples both in 3% (w/v) (Fig. 1b) and 5% (w/v) carob flour concentration. Electrospinning potential of conventionally heated solutions were quite different than microwave-heated ones. This could be explained by the differences in the mechanism of conventional and microwave heating.

To enlighten the reason of difference in morphology of microwave and conventionally treated samples, free amino groups were determined. There was no significant difference between the unheated solution and conventionally heated one in terms of free amino groups, which had $0.0332 \pm 0.0075$ and $0.0354 \pm 0.0011$ g/100 mL, respectively. On the other hand, sample treated by microwave heating for 2.5 min had the highest amount of available free amino group ($0.0426 \pm 0.0047$ g/100 mL) as compared with the conventionally heated samples ($0.0354 \pm 0.0011$ g/100 mL). In microwave heating, there is internal heat generation, which increases the internal pressure in the sample (Sumnu 2001). This internal pressure gradient might have increased the release of free amino groups from the sample. Moreover, microwave heating might have a different effect on the protein molecules. Microwave heating can facilitate protein unfolding, which can be linked to excitation of collective intrinsic modes in the proteins (Bohr and Bohr 2000).

In this context, it was clear that microwave heating had a significant effect on obtaining bead-free fibers due to the release of amino groups. It was worth to investigate how free amino acid could affect elecrospinnability. This could be related to the viscosity of the solutions. Increasing number of amino groups were shown to increase viscosity of solutions. Viscosity values of microwave treated samples were determined as 0.163 Pa s. This value was 0.138 Pa s for conventionally heated sample. This showed that the increase in free amino group could be related to increase in viscosity values. The increase in viscosity enhanced elecrospinnability of solutions, thus bead-free and homogeneous structures were obtained. In electrospinning process, optimum viscosity value of the solutions is considered as a key parameter to obtain homogeneous and bead free nanofibers (Liu et al. 2017).

To observe the effect of starch on fiber morphology, different concentrations of rice starch from 0.25 to 0.75% were added to the solutions. In microwave heating method, maximum concentrations to obtain homogenous fibers were determined as 5% carob flour and 0.75% rice starch. In conventional heating method, by adding 0.5% starch to 3% carob flour, bead-free nanofiber could be obtained. As discussed before, without addition of rice starch, bead-free and homogeneous fibers could not be achieved in conventionally heated samples (Fig. 1a). The reason could be linked to the effect of amylose content on elecrospinnability. Higher amylose content is very effective on formation of homogenous fibers during electrospinning (Wang et al. 2018). Addition of rice
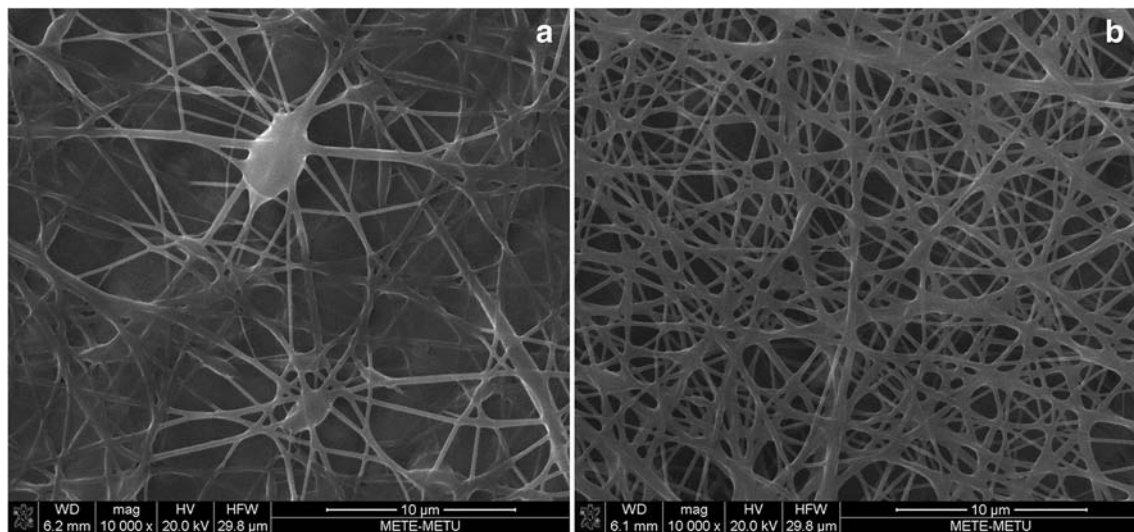
Fig. 1 SEM images of electrospun nanofibers containing 3% carob flour **a** treated by conventional heating and **b** treated by microwave heating

starch helped to obtain homogeneous and bead-free fiber formation in conventionally heated solutions (Fig. 2). For conventional heating, 3% flour and 0.5% starch combination were the lowest possible concentration for homogeneous and bead-free fiber formation. Thus, solutions containing carob flour of 3% concentration and starch of 0.5% concentration were selected in order to compare microwave and conventional heating. Viscosity and electrical conductivity of the solutions were determined since they are important parameters for electrospinning process.

Table 1 shows the viscosity and electrical conductivity of the solutions and average diameter values of the fibers. All the solutions showed Newtonian behavior obeying Newton's law of viscosity with high coefficient of determination value ($R^2 =$ 0.99). According to the results, M-3F-0.5S sample had the highest viscosity value as compared with the other samples ($p \leq 0.05$). C-3F-0.5S sample had lower viscosity value than M-3F-0.5S sample. This can be related to the free amino group content. As discussed before, according to OPA analysis results, microwave-heating process increased the release of free amino group in comparison with conventional heating. At that point, it was found that there was a correlation between increase in free amino acid content and increase in viscosity. Viscosity increase was mainly resulted from increased resistance offered by the more structured solvent caused by increase of moving amino group part. Thus, solvation effects could also contribute to movement of amino groups (Yan et al. 2002; Ali et al. 2010). Thereby, viscosity difference between conventionally heated and microwave-heated sample could be explained by the available amino group amount in the solutions. When the starch effect was considered, it was found that viscosity of M-5F-0.5S and M-5F-0S samples were not significantly different from each other. The reason could be that starch amount was not sufficient to cause a significant change in viscosity. In addition to these measurements, to

confirm the importance of viscosity, viscosity of conventionally heated solution with 5% of carob flour concentration was measured and was found as 0.128 Pa s, which was significantly lower than those of the other samples ($p \leq 0.05$). It was already mentioned that conventionally heated sample with 5% carob flour resulted in nonhomogeneous nanofibers with beads. In this regard, it can be concluded that lower viscosity values resulted in nonhomogeneous fibers with beads.

Electrical conductivity is an important factor in electrospinning process. It is known that electrical conductivity is related to movement of charges, which is important to overcome surface tension forces to start spinning process (Vega-Lugo and Lim 2012). For example, high conductivity can cause greater electrostatic repulsion force, thus better stretching properties, which are responsible for inducing the bending instability and stretching (Vega-Lugo and Lim 2012).

In Table 1, it was clear that M-3F-0.5S and C-3F-0.5S samples had significantly lower conductivity values than M-5F-0S and M-5F-0.5S samples ($p \leq 0.05$). This can be correlated to pH adjustment of the solutions. To adjust pH of the solutions to 10, NaOH solution was added. Thus, number of charged molecules increased by the presence of $Na^+$ and $OH^-$ ions. This directly related to electrical conductivity increase. For 5% solutions, since more NaOH solution is required to adjust pH, higher conductivity values were obtained.

There was no significant effect of heating treatment difference on electrical conductivity since M-3F-0.5S and C-3F-0.5S samples had the same electrical conductivity value (Table 1).

Figure 2 shows the SEM images and diameter distributions of films obtained from solutions containing different concentrations of flour, starch, and heating processes. Also, average fiber diameter and standard deviation results are available. Range of average fiber diameters was between 220 and 300 nm. In M-3F-0.5S sample, the most uniform distribution

**Fig. 2** SEM images and diameter distributions of the films obtained from different solutions with different concentrations and heating processes. **a** M-5F-0.5S, **b** M-5F-0S, **c** M-3F-0.5S, and **d** C-3F-0.5S
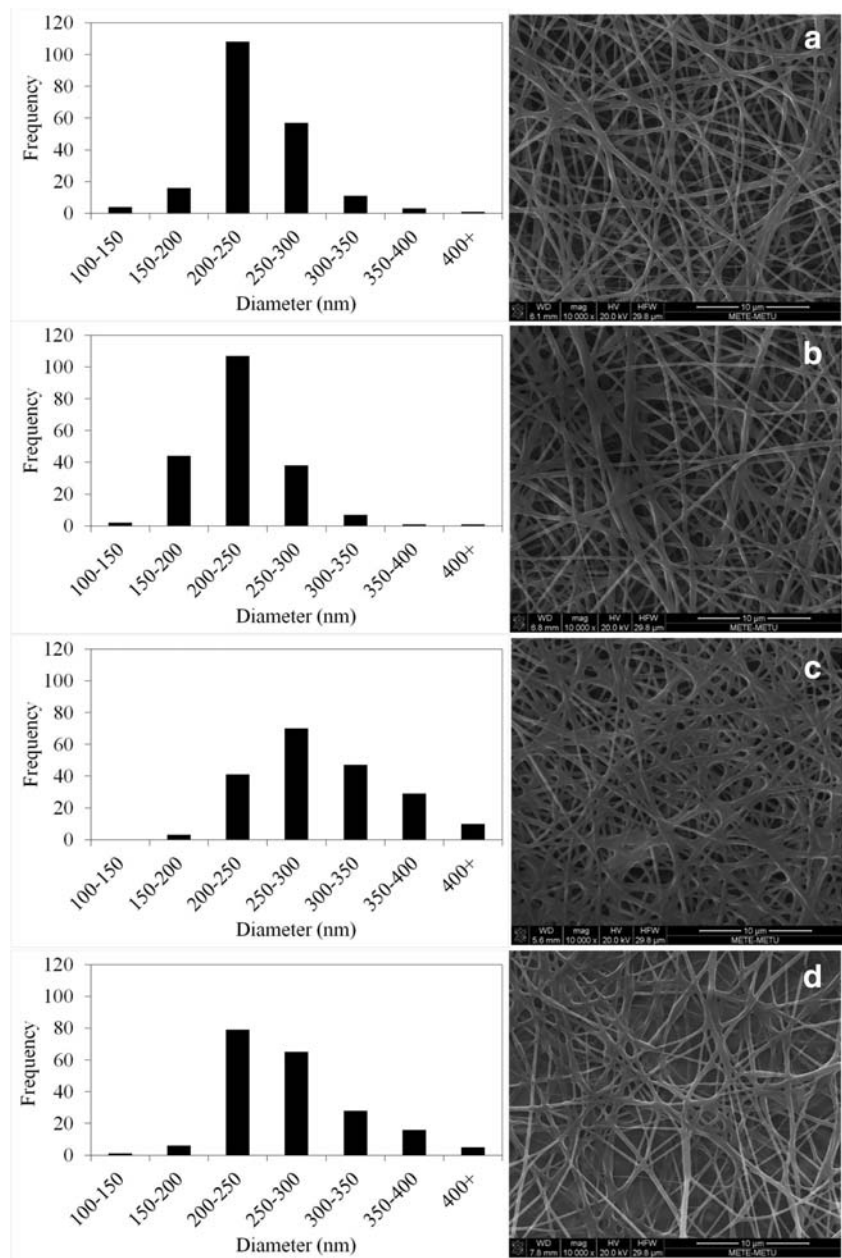


can be seen, while M-5F-0.5S, M-5F-0S, and C-3F-0.5S samples showed more uneven distributions. Table 1 shows the average fiber diameter of the films. It can be concluded that

M-3F-0.5S sample had the largest diameter. Viscosity and electrical conductivity are considered as one of the most effective parameters that can affect fiber diameter (Hu et al.

**Table 1** Viscosity and electrical conductivity values of the solutions and average diameters of the fibers

| Sample | Viscosity (Pa s) | Electrical conductivity (mS.cm$^{-1}$) | Average fiber diameter (nm) |
|---|---|---|---|
| M-5F-0.5S | 0.166 ± 0.001b* | 2.710 ± 0.042a | 243.68 ± 0.25c |
| M-5F-0S | 0.153 ± 0.008bc | 2.380 ± 0.007b | 228.34 ± 4.26c |
| M-3F-0.5S | 0.239 ± 0.005a | 1.504 ± 0.003c | 301 .53 ± 0.36a |
| C-3F-0.5S | 0.146 ± 0.001c | 1.563 ± 0.002c | 274.87 ± 0.79b |

*Columns with different lowercase letters are significantly different ($p \leq 0.05$)

2014). A correlation was found between viscosity and fiber diameter in previous studies (Moomand and Lim 2015). As viscosity value of zein-ethanol mixed solutions increased, a significant increase in fiber diameter of their films and minimal bead formation was observed. In addition, it was observed that the increase in electrical conductivity of the solution could result in a decrease in fiber diameter (Tavassoli-Kafrani et al. 2018). The reason could be linked to difficult elongation of jet. Low values of conductivity cause insufficient elongation, thus higher fiber diameter size (Bhardwaj and Kundu 2010). According to the viscosity and electrical conductivity results of this study, M-3F-0.5S sample had the highest viscosity and the lowest conductivity values. For that reason, it was expected for this sample to have the highest fiber diameter.

C-3F-0.5S sample had the second biggest diameter. This could be associated with its lower viscosity value as compared with M-3F-0.5S sample, although their electrical conductivity values were not significantly different than each other. At that point, viscosity was found to be a more effective parameter on fiber diameter rather than electrical conductivity. In 5% flour containing samples (M-5F-0.5S, M-5F-0S), it was observed that they had the lowest fiber diameters as compared with 3% flour containing samples. Again, this could be reasoned with their lower viscosity values and also their quite high electrical conductivity values. Both viscosity and electrical conductivity resulted in a decrease in fiber diameter.

## Characterization of Nanofibers

Nanofibers of M-5F-0.5S, M-5F-0S, M-3F-0.5S, and C-3F-0.5S were characterized by using WVP, X-ray diffraction, mechanical test, DSC, and FTIR analysis.

### WVP

In fiber characterization, WVP is one of the most important criteria due to its impact on moisture transfer through the film. Lower WVP values are more preferable in terms of packaging purposes since lower values refer to less amount of moisture transferring to the environments.

In Table 2, WVP values of films were shown. Although these values were slightly higher than that of synthetic

polymers LDPE ($0.36 \times 10^{-12}$ g m$^{-1}$ s$^{-1}$ Pa$^{-1}$) (He and Hwang 2016), they were lower than biodegradable PLA film ($26.02 \times 10^{-12}$ g m$^{-1}$ s$^{-1}$ Pa$^{-1}$) (Aydogdu et al. 2019b), cellulose-based polymer package, cellophane, ($0.84 \times 10^{-10}$ g m$^{-1}$ s$^{-1}$ Pa$^{-1}$) (Mali et al. 2002), and rice flour–cellulose fiber films ($0.313 \times 10^{-10}$ g m$^{-1}$ s$^{-1}$ Pa$^{-1}$) (Dias et al. 2011). In the literature, there are a couple of ways to lower WVP of hydrophilic films, such as the addition of lipids (Acosta et al. 2015), crossing-linking agents, and film processing (Choi et al. 2018). Therefore, comparing with the literature results, although film materials had similar characteristics, electrospun nanofiber films had lower values as compared with films made by the casting method. This was one of the advantages of electrospinning. Electrospun nanofilm was formed by the deposition of nanofibers on each other and form compact layers. In this study, the thickness of films was recorded as approximately 0.04 mm ± 0.001 mm and fiber diameter was nearly 262 ± 16 nm. Therefore, more than 150 nanofibers layered out each other. This structure formed a torturous path and made it difficult for transfer of water vapor. In this way, the permeability of nanofilms decreased.

A similar finding was also observed for PEO, HPMC, and lentil flour electrospun nanofibers. In this study, depending on pea flour concentration of the film, WVP values were $1.218 \times 10^{-12}$ g m$^{-1}$ s$^{-1}$ Pa$^{-1}$ and $1.754 \times 10^{-12}$ g m$^{-1}$ s$^{-1}$ Pa$^{-1}$ (Oguz et al. 2018). Furthermore, it is worth to notice that the reason of small variation between carob flour and pea flour nanofilms might be due to variation of polar amino acid content and amylose-amylopectin content of the flours.

Microwave treatment is another factor affecting WVP. Although films had the same formulations (M-3F-0.5S and C-3F-0.5S), microwave treated samples had significantly lower WVP than conventionally treated ones. In fact, the aim of addition NaOH to solutions was to adjust pH 10 and to denature the proteins to make it more spinnable. However, it was recorded that alkali treatment was also used to modify the gelatinization process of starches. Disruption of intra and inter hydrogen bonding between amylose and amylopectin molecules led to decreasing of gelatinization temperature (Marques et al. 2006). Due to the internal heat generation principle of the microwave, starch granules became more damaged and disordered (Zhao et al. 2019). This working principle also resulted

**Table 2** Water vapor permeability and mechanical properties of films

| Sample | WVP × 10$^{-12}$ (g s$^{-1}$m$^{-1}$Pa$^{-1}$) | Tensile strength (N) | Young modulus (N m$^{-1}$) | Elongation at break (%) |
|---|---|---|---|---|
| M-5F-0.5S | 2.32 ± 0.03b* | 0.955 ± 0.032c* | 29.55 ± 1.57b* | 41.36 ± 0.76b* |
| M-5F-0S | 2.73 ± 0.06a | 0.625 ± 0.053c | 22.27 ± 1.47b | 34.99 ± 0.67b |
| M-3F-0.5S | 1.68 ± 0.02c | 3.875 ± 0.088a | 79.91 ± 2.48a | 61.25 ± 3.21a |
| C-3F-0.5S | 2.13 ± 0.01b | 2.305 ± 0.004b | 69.784 ± 0.42a | 41.69 ± 0.76b |

*Columns with different lowercase letters are significantly different ($p \leq 0.05$)

in puffing of starch, which might accelerate the chemical re-action. Furthermore, electromagnetic waves caused polarization and alignment of macromolecules under the field, which might cause breakage of hydrogen bonds (Shi et al. 2014). To adjust pH to 10, more NaOH solution was added to M-5F-0.5S compared with C-3F-0.5S. The addition of more alkali solution and microwave treatment might accelerate bond formation between PEO, carob flour, and starch molecules. By the way, more linkage and the more homogenous solution might cause the formation of less permeable nanofilm. Thus, different results between M-3F-0.5S and C-3F-0.5S could be explained by microwave effect.

Permeability difference between M-3F-0.5S and C-3F-0.5S might also be explained by fiber diameter difference. M-3F-0.5S sample had quite a larger fiber diameter compared with C-3F-0.5S sample (Table 1). It was shown in a previous study that increase in fiber diameter had a decreasing effect on the porosity of films; thereby, as fiber diameter increases, the porosity of films decreased (Juklíčková et al. 2012). The decrease in porosity was more desirable in terms of reducing water vapor transfer. The same observation was also valid for M-5F-0.5S and M-3F-0.5S samples. Although both samples were treated with microwave and M-5F-0.5S had higher carob flour, the higher fiber diameter of M-3F-0.5S strongly decreased WVP.

### XRD

In addition to these, crystallinity might be another factor that strongly affects permeability characteristics of films. Higher intensity of peaks was interpreted as higher crystallinity. Figure 3 shows XRD results of the films from different solutions, concentrations, and heating processes. M-3F-0.5S sample had the highest crystallinity and the lowest permeability. On the other hand, M-5F-0S had the lowest crystallinity and highest permeability. XRD pattern of other samples also showed similar correlation with WVP. In crystal regions, molecules had higher density and more compact characteristic, and molecule alignments were more regular, but in amorphous phases, they were less dense. Therefore, due to crystal

structure and regular molecule orientation, water molecule passage through crystal parts was relatively slow. Similarly, in the literature, chitosan was blended with different compounds, namely, whey protein concentrate, lactoferrin, and glycomacropeptide, and their packaging film was analyzed in terms of barrier properties. Results were revealed that depending on protein type, crystallinity of films showed differences. Film having higher degree in crystallinity showed lower WVP. Finally, it was recorded that permeability was a primary function of the amorphous phase (Bourbon et al. 2011). In the literature, it was recorded that higher crystallinity improved barrier property of film since crystal structure was an inert and impermeable character. Therefore, diffusion of molecules could take place mainly in amorphous regions (Fabra et al. 2013). Since PEO is a semicrystalline polymer, it has diffraction peaks at $2\theta = 19°$ and $23°$ (Uyar and Besenbacher 2009). As can be seen in the Fig. 3, XRD patterns of nanofilms were very similar to PEO and no peak observed were distinct from the PEO pattern. These structures showed that both carob flour and rice starch were homogenously distributed through the carrier polymer. They did not show any unique crystal formation. This also showed how materials interacted strongly with each other.

### Mechanical Properties

Mechanical properties of nanofibers depend on some parameters such as composition, processing condition, fiber diameter, distribution, and interaction between components (Sengupta et al. 2007). Tensile strength, Young's modulus, and elongation at break values of films were given in Table 2.

XRD results and mechanical properties of the films complemented each other. Fibers with high peak intensity were regarded as more crystal structure with a numerous hydrogen bonding and more molecular orientation. It should be noticed that tensile strength of the films was aligned in an order of peak intensity values. Therefore, increasing crystallinity promoted tensile strength of the films.

Films with relatively high crystallinity not only had higher tensile strength but also higher Young's modulus because of



**Fig. 3** XRD results of electrospun nanofilms
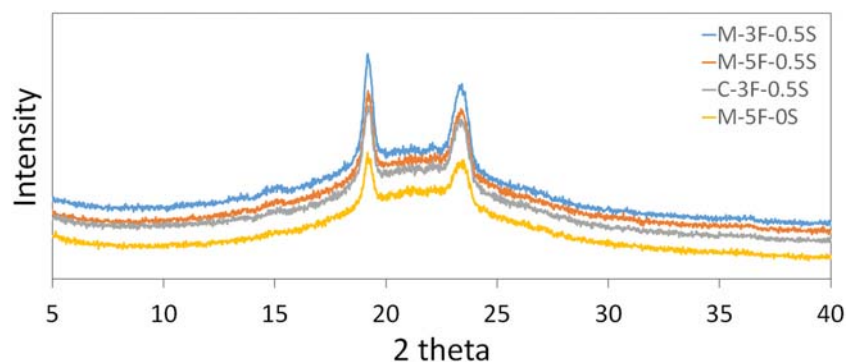
the same reasons, high hydrogen bonding, and more compact, rigid structure. These results were also supported by other studies. It was recorded that films with a compact structure and higher degree in crystallinity had higher elastic modulus and tensile strength. Although crystal structure was less in quantity than the amorphous phase, relative increase in crystallinity showed an increasing trend on strength of film (Fabra et al. 2013).

Fiber diameter of the film seemed to be correlated with mechanical properties. Increasing fiber diameter increased tensile strength of the films. For example, M-3F-0.5S sample had the highest fiber diameter and tensile strength. M-5F-0.5S and M-5F-0S sample had smaller diameter with a low tensile strength.

Films containing 5% carob flour had lower tensile strength values. In the literature, hydrophobic molecules present in the film formed clusters in the matrix and decreased tensile strength by weakening bond interactions (Sivarooban et al. 2008). Increasing carob flour concentration also increased hydrophobic protein or amino acids amount in the film forming solution. Therefore, these molecules might form aggregates and act as an impurity that decreased mechanical properties.

It was also recorded that tea polyphenol added polylactic acid (PLA) fibers had lower elongation at break and tensile strength. Presence of tea polyphenols reduced stretching ability of PLA chains by restricting PLA molecule bonding (Liu et al. 2018). Hydrophobic molecules might have the same effect for higher carob flour containing samples. In addition to that, these aggregates might disturb equal force distribution on fibers.

## DSC Analysis

In Table 3, glass transition temperatures ($T_g$), melting temperatures ($T_m$), and melting enthalpies ($\Delta H_m$) of the films are shown. In addition to these measurements, pure PEO was also tested in DSC. Although melting point of pure PEO was found as 71.5 °C, films had lower melting points, which were around 58 °C. The reason of this depression in $T_m$ might be the

disruption of crystal structure of PEO end of the interaction with carob flour and rice starch. Similar findings were also reported for gallic acid–loaded lentil flour–PEO nanofibers. Melting temperatures of PEO and the nanofilms were recorded as 68 °C and 62 °C, respectively. This indicated similarly that gallic acid and lentil flour obstructed regular crystal structure of PEO (Aydogdu et al. 2019a). Furthermore, after ejection of solution from tip of the needle to the collector plate, solvent evaporation occurs very fast. During this process, both elongation of polymers and solidification might also cause a change in crystallinity (Aydogdu et al. 2018a).

Melting is a phenomenon that is valid for crystalline polymers. When original crystal structure of polymer is damaged, it requires less energy to melt. Enthalpy of melting of 5% flour containing samples was lower than that of 3% flour containing ones. As carob flour and rice starch concentration increased, $\Delta H_m$ value decreased. Similar to melting point results, the reason could be linked to depression of crystalline structure of PEO due to interactions with biopolymer content. These results were also correlated with the literature. For example, thermal analysis of nanofibers made up of poly (ε-caprolactone) (PCL) and fish sarcoplasmic protein (FSP) indicated that 8% addition of FSP to PCL polymer decreased melting enthalpy of pure PCL nanofiber about 63% (Sahin et al. 2018).

Glass transition temperature is a point at which transition between glassy state to rubbery state occurs (Saba et al. 2017). $T_g$ decreases with increasing chain mobility of polymers. In glass transition temperature results, M-5F-0S and M-5F-0.5S samples had higher $T_g$ values compared with M-3F-0.5S and C-3F-0.5S samples. Increasing biopolymer concentration might increase water insoluble materials such as fibers and proteins in electrospinning solutions. These insoluble compounds might decrease free volume of polymer and chain mobility. By the way, this might be ending up with increasing $T_g$. Since nanofibers have both $T_m$ and $T_g$ value, they are semicrystal materials.

## FTIR Analysis

FTIR spectrum of nanofibers, PEO, carob flour, and rice starch are shown in Fig. 4. Generally, in FTIR spectrum, it was described as 800–1600 cm$^{-1}$ (the fingerprint region), the region between 2800 and 3000 cm$^{-1}$ (CH stretch region), and the region between 3000 and 3600 cm$^{-1}$ (OH stretch region) (Aydogdu et al. 2019a). Samples showed characteristic peak of pure components, which was supporting presence of these three constituents in the nanofibers, and well interaction between each other. Nanofibers and PEO showed similar peak at position 840 cm$^{-1}$, which was due to C-O stretching, C-C stretching, and CH$_2$ rocking (Pielichowski and Flejtuch 2005). Peaks located at 1058, 1095, and 1145 cm$^{-1}$ come from characteristic peak of pure PEO, which was linked to

**Table 3** Thermal properties of the samples

| Sample | $T_g$ (°C) | $T_m$ (°C) | $\Delta H_m$ (J g$^{-1}$) |
|---|---|---|---|
| M-5F-0.5S | −13.58 ± 0.11a | 58.66 ± 0.11a | 29.41 ± 0.35b |
| M-5F-0S | −12.83 ± 0.04a | 58.17 ± 0.03a | 30.09 ± 1.02b |
| M-3F-0.5S | −14.45 ± 0.02b | 58.57 ± 0.10a | 38.80 ± 0.65a |
| C-3F-0.5S | −14.73 ± 0.18b | 58.25 ± 0.02a | 38.39 ± 0.98a |

Columns with different lowercase letters are significantly different ($p \leq 0.05$)

$T_g$ glass transition temperature, $T_m$ melting temperature, $\Delta H_m$ melting enthalpy

**Fig. 4** FTIR spectra of nanofibers FTIR spectra of **a** M-5F-0.5S, M-5F-0S, M-3F-0.5S, and C-3F-0.5S samples, **b** FTIR spectra of PEO, **c** FTIR spectra of carob flour, **d** FTIR spectra of rice starch
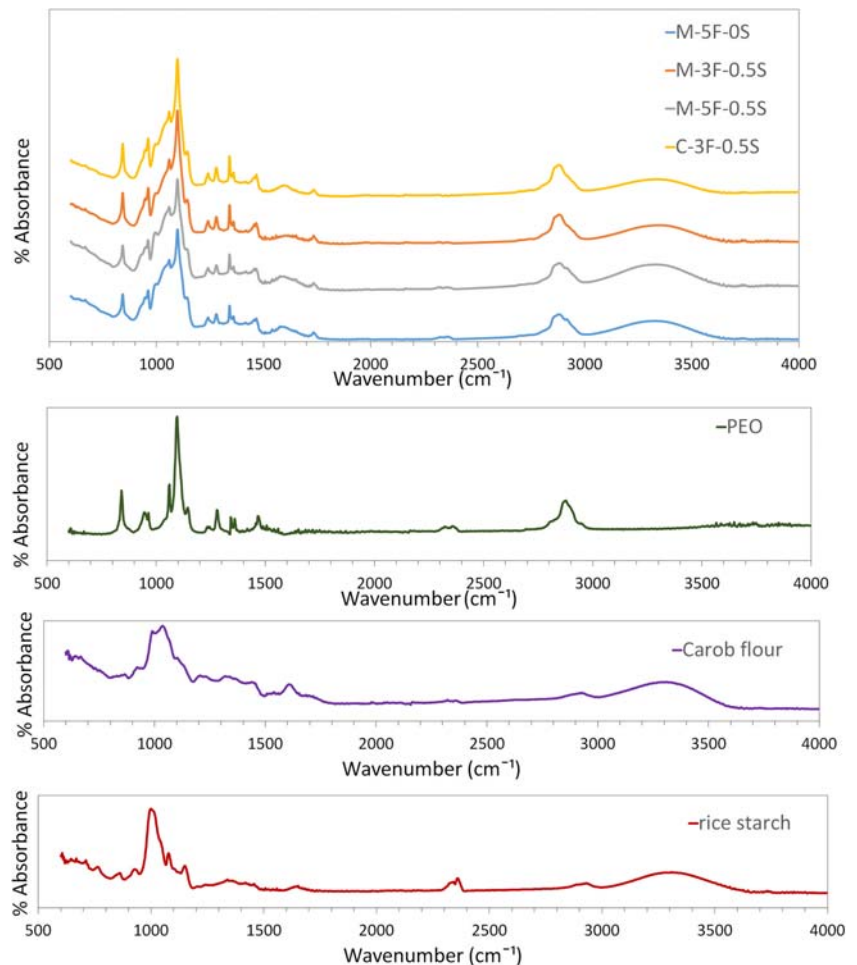


stretching vibrations of the ether bond or C-O-C complex (Fig. 4a, b). The other peaks that are located around 1280, 1340, and 1467 $cm^{-1}$ are related with PEO, which are characteristics of $CH_2$ twisting, $CH_2$ wagging, and $CH_2$ scissoring, respectively (Aydogdu et al. 2018b). Actually, absorptions peaks at 1145 and 1058 $cm^{-1}$ were related to crystallinity of PEO (Sim et al. 2010). After thermal and chemical treatment and electrospinning process, it was expected to reduction in intensity. Although starch and carob flour has also crystal starch components, after heat treatment, they might lose mostly their original structure. Therefore, although PEO crystallinity remains unchanged, compared with increasing concentration of the amorphous part caused to such a spectrum.

At fingerprint region, overlapping and complex spectra made difficult attribution of exact band assignment. In this part, spectra were based on vibrational form of monomer glucose units of starch, cellulose, amylose, and amylopectin. Peaks positioned at 960 $cm^{-1}$ in spectra of nanofibers was attributed to vibrations arising from C-O-C of $\alpha$-1,4 glycosidic linkages (Kizil et al. 2002). Presence of peak at only nanofibers spectrum with a high peak intensity proved strong

interaction between components and new bond formation. The peaks at 1242 $cm^{-1}$ corresponded to $CH_2OH$ related mode besides the C-O-H deformation mode (Kizil et al. 2002). Small peaks located at 1600–1700 $cm^{-1}$ and 1531 $cm^{-1}$ regions were observed in both carob flour, starch, and nanofibers spectrums, which are related to proteins and peptides and characteristic peaks of Amide-I and Amide-II (Mamone et al. 2019). Carob flour was composed of both starch and protein, and trace amount of protein present in starch might lead to such a spectra. However, presence of peaks in nanofibers might be interpreted as more heat stable proteins. For example, proteins in the form of $\beta$-sheet had more thermally stable structure than $\alpha$-helix, $\beta$-turn, and unordered conformations (Mamone et al. 2019). Therefore, applied heat treatment might not be enough for disrupting the secondary structure of some proteins. Furthermore, quaternary or tertiary structure of protein was more prone to be affected form heat treatments. Because of that, some proteins might lose their original conformation and have a secondary structure after treatments. Therefore, these peaks might belong to them also.

Peaks between 3000 and 2840 cm$^{-1}$ region was due to C-H stretching in alkenes (Manoj and Kunjomana 2012). Broad range peak between 3500 and 3300 cm$^{-1}$ was attributed to hydroxyl (OH) group (Chuai et al. 2001).

## Conclusions

In this study, it was illustrated that by microwave heating method, it was possible to produce bead-free and homogeneous electrospun nanofibers with various carob flour concentrations. The positive effect of microwave on electrospinning was explained by the increase in the free amino groups in the electrospinning solution. Thus, usage of microwaves as a pretreatment of electrospinning resulted in good film characteristics. Microwave-treated samples showed better film characteristics in terms of higher mechanical properties and lower water vapor permeability as compared with conventionally treated sample. Furthermore, it was possible to obtain nanofibers with better mechanical properties by incorporation of rice starch to carob flour. Films with relatively high crystallinity not only had higher tensile strength but also higher Young's modulus. Fiber diameter of the film seemed to be correlated with mechanical properties. Increasing fiber diameter increased tensile strength of the films. M-3F-0.5S sample can be suggested to be used in food packaging by its better mechanical properties and higher viscosity. To conclude, microwave heating method can be a promising method to be used in food packaging.

## References

Acosta, S., Jiménez, A., Cháfer, M., González-Martínez, C., & Chiralt, A. (2015). Physical properties and stability of starch-gelatin based films as affected by the addition of esters of fatty acids. *Food Hydrocolloids, 49*, 135–143. https://doi.org/10.1016/j.foodhyd.2015.03.015.

Ali, A., Shahjahan, & Ansari, N. H. (2010). Density and viscosity of α-amino acids in aqueous solutions of cetyltrimethylammonium bromide. *Russian Chemical Bulletin, 59*(10), 1999–2004. https://doi.org/10.1007/s11172-010-0346-2.

Aydogdu, A., Sumnu, G., & Sahin, S. (2018a). A novel electrospun hydroxypropyl methylcellulose/polyethylene oxide blend nanofibers: Morphology and physicochemical properties. *Carbohydrate Polymers, 181*(June 2017), 234–246. https://doi.org/10.1016/j.carbpol.2017.10.071.

Aydogdu, A., Sumnu, G., & Sahin, S. (2018b). A novel electrospun hydroxypropyl methylcellulose/polyethylene oxide blend nanofibers: Morphology and physicochemical properties. *Carbohydrate Polymers, 181*(June 2017), 234–246. https://doi.org/10.1016/j.carbpol.2017.10.071.

Aydogdu, A., Yildiz, E., Aydogdu, Y., Sumnu, G., Sahin, S., & Ayhan, Z. (2019a). Enhancing oxidative stability of walnuts by using gallic acid loaded lentil flour based electrospun nanofibers as active packaging material. *Food Hydrocolloids, 95*(April), 245–255. https://doi.org/10.1016/j.foodhyd.2019.04.020.

Aydogdu, A., Yildiz, E., Ayhan, Z., Aydogdu, Y., Sumnu, G., & Sahin, S. (2019b). Nanostructured poly(lactic acid)/soy protein/HPMC films by electrospinning for potential applications in food industry. *European Polymer Journal, 112*(January), 477–486. https://doi.org/10.1016/j.eurpolymj.2019.01.006.

Bhardwaj, N., & Kundu, S. C. (2010). Electrospinning: a fascinating fiber fabrication technique. *Biotechnology Advances, 28*(3), 325–347. https://doi.org/10.1016/j.biotechadv.2010.01.004.

Bohr, H., & Bohr, J. (2000). Microwave-enhanced folding and denaturation of globular proteins. *Physical Review E - Statistical Physics, Plasmas, Fluids, and Related Interdisciplinary Topics, 61*(4), 4310–4314. https://doi.org/10.1103/PhysRevE.61.4310.

Bourbon, A. I., Pinheiro, A. C., Cerqueira, M. A., Rocha, C. M. R., Avides, M. C., Quintas, M. A. C., & Vicente, A. A. (2011). Physico-chemical characterization of chitosan-based edible films incorporating bioactive compounds of different molecular weight. *Journal of Food Engineering, 106*(2), 111–118. https://doi.org/10.1016/j.jfoodeng.2011.03.024.

Buffler, C. (1993). *Microwave cooking and processing*. New York: Springer UK.

Choi, I., Lee, S. E., Chang, Y., Lacroix, M., & Han, J. (2018). Effect of oxidized phenolic compounds on cross-linking and properties of biodegradable active packaging film composed of turmeric and gelatin. *Lwt, 93*(March), 427–433. https://doi.org/10.1016/j.lwt.2018.03.065.

Chuai, C., Almdal, K., Poulsen, L., & Plackett, D. (2001). Conifer fibers as reinforcing materials for polypropylene-based composites. *Journal of Applied Polymer Science, 80*(14), 2833–2841. https://doi.org/10.1002/app.1400.

Dias, A. B., Müller, C. M. O., Larotonda, F. D. S., & Laurindo, J. B. (2011). Mechanical and barrier properties of composite films based on rice flour and cellulose fibers. *LWT - Food Science and Technology, 44*(2), 535–542. https://doi.org/10.1016/j.lwt.2010.07.006.

Fabra, M. J., Lopez-Rubio, A., & Lagaron, J. M. (2013). High barrier polyhydroxyalcanoate food packaging film by means of nanostructured electrospun interlayers of zein. *Food Hydrocolloids, 32*(1), 106–114. https://doi.org/10.1016/j.foodhyd.2012.12.007.

Fabra, M. J., López-rubio, A., & Lagaron, J. M. (2015). Three-layer films based on wheat gluten and electrospun PHA. *Food and Bioprocess Technology, 8*, 2330–2340. https://doi.org/10.1007/s11947-015-1590-0.

Hadad, S., Amir, S., & Goli, H. (2019). Improving oxidative stability of flaxseed oil by encapsulation in electrospun flaxseed mucilage nanofiber. *Food and Bioprocess Technology, 12*, 829–838.

He, X., & Hwang, H. M. (2016). Nanotechnology in food science: functionality, applicability, and safety assessment. *Journal of Food and Drug Analysis, 24*(4), 671–681. https://doi.org/10.1016/j.jfda.2016.06.001.

Hu, X., Liu, S., Zhou, G., Huang, Y., Xie, Z., & Jing, X. (2014). Electrospinning of polymeric nanofibers for drug delivery applications. *Journal of Controlled Release, 185*(1), 12–21. https://doi.org/10.1016/j.jconrel.2014.04.018.

Juklíčková, M., Kubinová, Š., Širc, J., Zajícová, A., Hobzová, R., Michálek, J., et al. (2012). Morphological characterization of nanofibers: methods and application in practice. *Journal of Nanomaterials, 2012*, 1–14. https://doi.org/10.1155/2012/327369.

Kizil, R., Irudayaraj, J., & Seetharaman, K. (2002). Characterization of irradiated starches by using FT-Raman and FTIR spectroscopy. *Journal of Agricultural and Food Chemistry, 50*(14), 3912–3918. https://doi.org/10.1021/jf011652p.

Lewandowicz, G., Fornal, J., & Walkowski, A. (1997). Effect of microwave radiation on physico-chemical properties and structure of potato and tapioca starches. *Carbohydrate Polymers, 34*(4), 213–220. https://doi.org/10.1016/S0144-8617(97)00091-X.

Li, D., & Xia, Y. (2004). Direct fabrication of composite and ceramic hollow nanofibers by electrospinning. *Nano Letters, 4*(5), 933–938. https://doi.org/10.1021/nl049590f.

Li, J. Y., & Yeh, A. I. (2001). Relationships between thermal, rheological characteristics and swelling power for various starches. *Journal of Food Engineering, 50*(3), 141–148. https://doi.org/10.1016/S0260-8774(00)00236-3.

Lim, S.-T., Jane, J.-L., Rajagopalan, S., & Seib, P. A. (1992). Effect of starch granule size on physical properties of starch-filled polyethylene film. *Biotechnology Progress, 8*(1), 51–57. https://doi.org/10.1021/bp00013a008.

Liu, G., Gu, Z., Hong, Y., Cheng, L., & Li, C. (2017). Electrospun starch nanofibers: recent advances, challenges, and strategies for potential pharmaceutical applications. *Journal of Controlled Release, 252*, 95–107. https://doi.org/10.1016/j.jconrel.2017.03.016.

Liu, Y., Liang, X., Wang, S., Qin, W., & Zhang, Q. (2018). Electrospun antimicrobial polylactic acid/tea polyphenol nanofibers for food-packaging applications. *Polymers, 10*(5). https://doi.org/10.3390/polym10050561.

Mali, S., Grossmann, M. V. E., Garcia, M. A., Martino, M. N., & Zaritzky, N. E. (2002). Microstructural characterization of yam starch films. *Carbohydrate Polymers, 50*(4), 379–386. https://doi.org/10.1016/S0144-8617(02)00058-9.

Mamone, G., Sciammaro, L., De Caro, S., Di Stasio, L., Siano, F., Picariello, G., & Puppo, M. C. (2019). Comparative analysis of protein composition and digestibility of Ceratonia siliqua L. and Prosopis spp. seed germ flour. *Food Research International, 120*(February), 188–195. https://doi.org/10.1016/j.foodres.2019.02.035.

Manoj, B., & Kunjomana, A. G. (2012). Chemical leaching of an Indian bituminous coal and characterization of the products by vibrational spectroscopic techniques. *International Journal of Minerals, Metallurgy, and Materials, 19*(4), 279–283. https://doi.org/10.1007/s12613-012-0551-0.

Marques, P. T., Pérégo, C., Le Meins, J. F., Borsali, R., & Soldi, V. (2006). Study of gelatinization process and viscoelastic properties of cassava starch: effect of sodium hydroxide and ethylene glycol diacrylate as cross-linking agent. *Carbohydrate Polymers, 66*(3), 396–407. https://doi.org/10.1016/j.carbpol.2006.03.028.

Mendes, A. C., Stephansen, K., & Chronakis, I. S. (2017). Electrospinning of food proteins and polysaccharides. *Food Hydrocolloids, 68*, 53–68. https://doi.org/10.1016/j.foodhyd.2016.10.022.

Moomand, K., & Lim, L. T. (2015). Properties of encapsulated fish oil in electrospun zein fibres under simulated in vitro conditions. *Food and Bioprocess Technology, 8*(2), 431–444. https://doi.org/10.1007/s11947-014-1414-7.

Müller, C. M. O., Laurindo, J. B., & Yamashita, F. (2009). Effect of cellulose fibers addition on the mechanical properties and water vapor barrier of starch-based films. *Food Hydrocolloids, 23*(5), 1328–1333. https://doi.org/10.1016/j.foodhyd.2008.09.002.

Nielsen, P. M., Petersen, D., & Dambmann, C. (2001). Improved method for determining food protein degree of hydrolysis. *Journal of Food Science, 66*(5), 642–646. https://doi.org/10.1111/j.1365-2621.2001.tb04614.x.

Oguz, S., Tam, N., Aydogdu, A., Sumnu, G., & Sahin, S. (2018). Development of novel pea flour-based nanofibres by electrospinning method. *International Journal of Food Science and Technology, 53*(5), 1269–1277. https://doi.org/10.1111/ijfs.13707.

Özcan, M. M., Arslan, D., & Gökçalik, H. (2007). Some compositional properties and mineral contents of carob (Ceratonia siliqua) fruit, flour and syrup. *International Journal of Food Sciences and Nutrition, 58*(8), 652–658. https://doi.org/10.1080/09637480701395549.

Pielichowski, K., & Flejtuch, K. (2005). Non-oxidative thermal degradation of poly(ethylene oxide): kinetic and thermoanalytical study. *Journal of Analytical and Applied Pyrolysis, 73*(1), 131–138. https://doi.org/10.1016/j.jaap.2005.01.003.

Saba, N., Safwan, A., Sanyang, M. L., Mohammad, F., Pervaiz, M., Jawaid, M., Alothman, O. Y., & Sain, M. (2017). Thermal and dynamic mechanical properties of cellulose nanofibers reinforced epoxy composites. *International Journal of Biological Macromolecules, 102*, 822–828. https://doi.org/10.1016/j.ijbiomac.2017.04.074.

Sahin, Y. M., Su, S., Ozbek, B., Yücel, S., Pinar, O., Kazan, D., et al. (2018). Production and characterization of electrospun fish sarcoplasmic protein based nanofibers. *Journal of Food Engineering, 222*, 54–62. https://doi.org/10.1016/j.jfoodeng.2017.11.013.

Sengupta, R., Chakraborty, S., Bandyopadhyay, S., Dasgupta, S., Mukhopadhyay, R., Auddy, K., & Deuri, A. S. (2007). The morphology and mechanical properties of sodium alginate based electrospun poly(ethylene oxide) nanofiber. *Polymer Engineering & Science, 47*, 21–25. https://doi.org/10.1002/pen.

Shi, H., Yin, Y., & Jiao, S. (2014). Preparation and characterization of carboxymethyl starch under ultrasound-microwave synergistic interaction. *Journal of Applied Polymer Science, 131*(20), 1–8. https://doi.org/10.1002/app.40906.

Sim, L. H., Gan, S. N., Chan, C. H., & Yahya, R. (2010). ATR-FTIR studies on ion interaction of lithium perchlorate in polyacrylate/poly(ethylene oxide) blends. *Spectrochimica Acta - Part A: Molecular and Biomolecular Spectroscopy, 76*(3–4), 287–292. https://doi.org/10.1016/j.saa.2009.09.031.

Sivarooban, T., Hettiarachchy, N. S., & Johnson, M. G. (2008). Physical and antimicrobial properties of grape seed extract, nisin, and EDTA incorporated soy protein edible films. *Food Research International, 41*(8), 781–785. https://doi.org/10.1016/j.foodres.2008.04.007.

Standard Test Methods for Water Vapor Transmission of Materials. (1995). *Standard Test Methods for Water Vapor Transmission of Materials, 1*, 1–8. http://www.arnisco.com/astm/PDF/E96.PDF. Accessed 10 July 2019

Sumnu, G. (2001). A review on microwave baking of foods. *International Journal of Food Science and Technology, 36*(2), 117–127. https://doi.org/10.1046/j.1365-2621.2001.00479.x.

Surov, O. V., Voronova, M. I., Afineevskii, A. V., & Zakharov, A. G. (2018). Polyethylene oxide films reinforced by cellulose nanocrystals: microstructure-properties relationship. *Carbohydrate Polymers, 181*(June 2017), 489–498. https://doi.org/10.1016/j.carbpol.2017.10.075.

Tam, N., Oguz, S., Aydogdu, A., Sumnu, G., & Sahin, S. (2017). Influence of solution properties and pH on the fabrication of electrospun lentil flour/HPMC blend nanofibers. *Food Research International, 102*(July), 616–624. https://doi.org/10.1016/j.foodres.2017.09.049.

Tavassoli-kafrani, E., Amir, S., Goli, H., & Fathi, M. (2018). Encapsulation of orange essential oil using cross-linked electrospun gelatin nanofibers. *Food and Bioprocess Technology, 11*, 427–434.

Uyar, T., & Besenbacher, F. (2009). Electrospinning of cyclodextrin functionalized polyethylene oxide (PEO) nanofibers. *European Polymer Journal, 45*(4), 1032–1037. https://doi.org/10.1016/j.eurpolymj.2008.12.024.

Vega-Lugo, A. C., & Lim, L. T. (2012). Effects of poly(ethylene oxide) and pH on the electrospinning of whey protein isolate. *Journal of Polymer Science, Part B: Polymer Physics, 50*(16), 1188–1197. https://doi.org/10.1002/polb.23106.

Wang, N., Gao, Y. Z., Wang, P., Yang, S., Xie, T. M., & Xiao, Z. G. (2016). Effect of microwave modification on mechanical properties and structural characteristics of soy protein isolate and zein blended film. *Czech Journal of Food Sciences, 34*(2), 180–188. https://doi.org/10.17221/442/2015-CJFS.

Wang, W., Wang, H., Jin, X., Wang, H., Lin, T., & Zhu, Z. (2018). Effects of hydrogen bonding on starch granule dissolution, spinnability of starch solution, and properties of electrospun starch fibers. *Polymer, 153*(June), 643–652. https://doi.org/10.1016/j.polymer.2018.08.067.

Yan, Z., Wang, J., & Lu, J. (2002). Viscosity behavior of some $\alpha$-amino acids and their groups in water-sodium acetate mixtures. *Biophysical Chemistry, 99*(3), 199–207. https://doi.org/10.1016/S0301-4622(02)00200-4.

Yousif, A. K., & Alghzawi, H. M. (2000). Processing and characterization of carob powder. *Food Chemistry, 69*(3), 283–287. https://doi.org/10.1016/S0308-8146(99)00265-4.

Zhao, B., Sun, S., Lin, H., Chen, L., Qin, S., Wu, W., et al. (2019). Physicochemical properties and digestion of the lotus seed starch-green tea polyphenol complex under ultrasound-microwave synergistic interaction. *Ultrasonics Sonochemistry, 52*(October 2018), 50–61. https://doi.org/10.1016/j.ultsonch.2018.11.001.

**Publisher's Note** Springer Nature remains neutral with regard to jurisdictional claims in published maps and institutional affiliations.